Available online at https://doi.org/10.36303/SATNT.2021cosaami.33
Conference of the South African Advanced Materials Initiative

Using site occupation disorder to build bulk structures of $Ni_{1-x}Al_x$

CJ Thesner[1], A Falch[2], CGCE van Sittert[1*]

[1] Applied Molecular Modelling Group, Research Focus Area: Chemical Resource Beneficiation (CRB), North-West University, Private Bag X6001, Potchefstroom 2520, South Africa
[2] Electrochemistry for Energy & Environment Group, Research Focus Area: Chemical Resource Beneficiation (CRB), North-West University, Private Bag X6001, Potchefstroom 2520, South Africa
Email: Cornie.VanSittert@nwu.ac.za

Abstract

Raney nickel shows potential as an electrocatalyst for the oxygen evolution reaction (OER). However, the catalytic activity of Raney nickel varies with its properties. These properties are related to the composition of the bimetallic precursor used to synthesise Raney nickel. The bimetallic precursor consists of a combination of bimetallic phases. Various studies have been done on the well-known bimetallic phases, namely, Ni_2Al_3, NiAl and $NiAl_3$. However, to get a more comprehensive understanding of the influence of the bimetallic precursor on the properties of Raney nickel, a larger spectrum of bimetallic phases needs to be evaluated. In this study, the Site Occupation Disorder (SOD) program was used to build solid-state structures (bimetallic phases) with various $Ni_{1-x}Al_x$ bimetallic ratios. These $Ni_{1-x}Al_x$ bimetallic phases were evaluated, and unique configurations for each $Ni_{1-x}Al_x$ bimetallic ratio were obtained. The unique configurations were geometrically optimised using the General Utility Lattice Program (GULP) at 0K. These optimised unique configurations were thermodynamically evaluated over a range of 0.1K – 1200K, and the most stable configurations with a probability higher than 10% were identified. This study found that the stable non-homogeneous configurations fall within a range of 20% - 80% Ni content. A weight average combination of these configurations of the bimetallic phases will produce a non-homogeneous precursor with an average Ni content of 20% - 80%, which is in close agreement with experimental results. The approach in this study enables researchers to obtain a larger, repeatable spectrum of bimetallic phases for the investigation of Raney nickel precursors.

Keywords: Site Occupation Disorder, General Utility Lattice Program, nickel, aluminium, bimetallic phases, Raney nickel

1. Introduction

The world is facing an energy and environmental crisis, which has led to a need to develop various alternative forms of energy production.[1,2,3] Hydrogen gas (H_2) has been identified as a clean, sustainable and highly energy-dense energy source. However, H_2 is not found naturally.[4] There are several methods to produce H_2. The most prominent methods include reforming natural gas, gasification of coal, and water electrolysis.[5,6] Water electrolysis is considered a highly sustainable and clean way to produce H_2 of high purity with only oxygen gas (O_2) as a by-product.[5-8]

Water electrolysis consists of two half-cell reactions: the OER and the hydrogen evolution reaction (HER).[8,9] Of these two reactions, the OER is the rate-determining reaction and therefore requires an efficient electrocatalyst.[7] Studies have shown that Raney nickel, a porous Ni structure, is a possible electrocatalyst for the OER in an alkaline environment.[9]

However, the activity and selectivity of Raney nickel vary with the morphological properties of the final synthesised Raney nickel. The morphological properties of Raney nickel are dependent on the synthesis method,[10-13] which is influenced by the composition of the bimetallic precursor and the final porous structure.[13-15] During the synthesis of Raney nickel, the primary metal (Ni) is combined with a secondary metal (usually zinc (Zn) or aluminium (Al)) to form a bimetallic precursor containing various bimetallic phases.[16,17] The secondary metal in the bimetallic precursor is more active towards the leaching than the Ni. Of the two secondary metals mentioned above, Al produced the best results in leachability without influencing Ni's integrity.[17,18]

The most studied $Ni_{1-x}Al_x$ bimetallic phases, both experimentally and computationally, are Ni_2Al_3, NiAl and $NiAl_3$. These studies usually started with a specific bimetallic phase within an alloy or a bimetallic precursor.[11,14,17,19,20] However, to get a more comprehensive understanding of the influence of the bimetallic precursor on the morphological properties of Raney nickel, a larger spectrum of bimetallic phases needs to be evaluated. The bimetallic phases could be evaluated separately or combined in one bimetallic precursor structure.

The SOD[21] program can be used for a more systematic approach to build and model a spectrum of $Ni_{1-x}Al_x$ bimetallic phases. This program utilises the site occupancy disorder phenomenon seen in solid-state chemistry.[21] In the SOD program, atoms of the secondary metal (Al) are systematically substituted into each of the available lattice spaces of the bulk structure of the pure primary metal (Ni), according to a pre-defined $Ni_{1-x}Al_x$ bimetallic ratio at 0K. This substitution leads to several configurations that are directly proportional to the size of the bulk structure. In order to reduce the number of configurations obtained, only the unique configurations are identified by applying a set of geometric operators (translation, rotation, and reflection) that work in conjunction with the symmetry of the crystal structure of the primary metal.

Each unique configuration is accompanied by a degeneracy value, Ωm, which is the number of symmetry-bound configurations identified in the larger bulk structure. These symmetry-bound configurations have the same energy due to similar atomic arrangements within the larger bulk structure. Only one of these symmetry-bound configurations is listed as output for the SOD program, namely the unique configuration.

The unique configurations were geometrically optimised at 0K using GULP to find the most stable geometric orientation for the configurations.[22,23] These optimised structures were submitted to thermodynamic calculations with statistical SOD. These calculations require an input file of temperatures at which the data should be calculated. The thermodynamic calculations include the Boltzmann probability distributions, the configurational entropy, and the enthalpy of mixing.

In this study, a larger spectrum of potential $Ni_{1-x}Al_x$ bimetallic phases that may influence the morphology and thus the synthesis and properties of Raney nickel were built using SOD.

2. Computational method

2.1 Configurations built with SOD

The face-centred cubic (fcc) unit cell for Ni, within the space group Fm-3m, was constructed using the following lattice parameters: *a, b,* and *c* of 3.524 Å, and cell angles of 90.0°.[24] The unit cell was expanded into a 2×2×1 supercell. The 2×2×1 cell contains 16 atoms, where each atom represents 6.25% of the cell. Using the SOD program at 0K resulted in numerous symmetry-bound configurations for a specific $Ni_{1-x}Al_x$ bimetallic phase. Symmetry operations reduced these symmetry-bound configures to unique configurations, which were geometrically optimised using GULP[23] with the interatomic many-body potentials from the Sutton-Chen library.[22] The Boltzmann probability distributions, the configurational entropy and enthalpy of mixing were calculated for a temperature range of 0.1K - 1200K, in steps of 100K.

2.2 Boltzmann probability distributions

The Boltzmann probability distribution was calculated using the following equation:[21]

$$P_m = \frac{1}{Z}\,\Omega_m e^{(-E_m/k_BT)} . \quad (1)$$

where m is the specific configuration, E_m is the configuration energy, Ω_m the configuration degeneracy showing the number of times the unique configuration is observed, k_B is Boltzmann's constant (8.6173×10^{-5} eV·K^{-1}), and Z is the partition function in the following equation:

$$Z = \sum_{m=1}^{N} e^{(-E_m/k_BT)} . \quad (2)$$

2.3 Stability of configurations

The stability of the configurations was determined by studying the entropy, which is calculated using the following equation:[21]

$$S_m = k_B T \ln \Omega_m , \quad (3)$$

where T is temperature, and the rest of the terms are as defined earlier.

The morphology of the various bimetallic phases could be explained by the enthalpy of mixing.[25]

$$\Delta H_{mix} = H[Ni_{1-x}Al_x] - (1-x)H[Ni] - xH[Al] , \quad (4)$$

where $H[Ni_{1-x}Al_x]$ is the enthalpy of a specific $Ni_{1-x}Al_x$ bimetallic phase, and H[Ni] and H[Al] are the enthalpies of the pure metals. The $H[Ni_{1-x}Al_x]$ can be calculated as a weight average from the configuration enthalpy:[21]

$$H[Ni_{1-x}Al_x] = \sum_{m=1}^{N} P_m H_m [Ni_{1-x}Al_x], \quad (5)$$

where $H_m[Ni_{1-x}Al_x]$ is the configuration enthalpy, and the rest of the terms are as defined earlier.

Table 1: The configurations for various $Ni_{1-x}Al_x$ bimetallic phases

Bimetallic phase	Total number of symmetry-bound configurations	Unique configurations	Unique configurations probable at 0K
$Ni_{15}Al_1$	16	1	1
$Ni_{14}Al_2$	120	5	1
$Ni_{13}Al_3$	560	10	1
$Ni_{12}Al_4$	1820	33	1
$Ni_{11}Al_5$	4368	53	1
$Ni_{10}Al_6$	8008	101	1
Ni_9Al_7	11440	122	1
Ni_8Al_8	12870	153	2
Ni_7Al_9	11440	122	1
Ni_6Al_{10}	8008	101	1
Ni_5Al_{11}	4368	53	1
Ni_4Al_{12}	1820	33	1
Ni_3Al_{13}	560	10	1
Ni_2Al_{14}	120	5	1
Ni_1Al_{15}	16	1	1

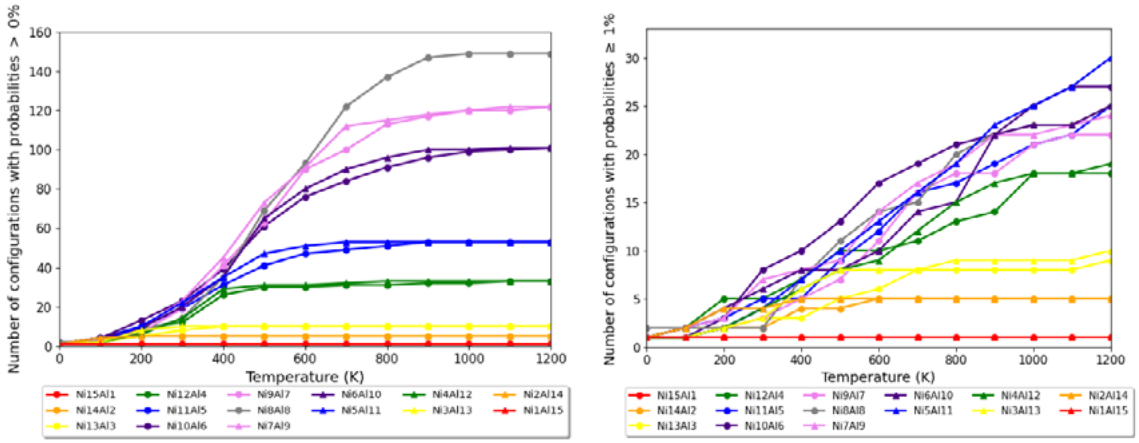

(a) (b)

Figure 1: The number of configurations for the $Ni_{1-x}Al_x$ bimetallic phases over a temperature range of 0.1K – 1200K for (a) existence probabilities > 0%, and (b) existence probabilities ≥ 1%. (Circle markers represent ratios where the Ni content is the highest, and triangle markers represent ratios where Al content is the highest.)

3. Results and Discussion

3.1 Configurations built with SOD

The total number of symmetry-bound configurations and the unique configurations for various $Ni_{1-x}Al_x$ bimetallic phases are listed in Table 1. For example, in the case of the 1:1 atomic ratio (bimetallic phase Ni_8Al_8), the total number of symmetry-bound configurations is 12870, of which only 153 configurations are unique. The number of configurations for all the bimetallic phases investigated is distributed symmetrically around the Ni_8Al_8 bimetallic phase. This distribution is observed since little or no influence outside the bulk structure (periodic supercell) was considered.

Initially, the various symmetry-bound configurations were built at 0K. However, Raney nickel is prepared at higher temperatures. Therefore, the temperature influence on the probability distribution was considered, and it was observed that the number of unique configurations increases as temperature increases.

3.2 Boltzmann probability distributions

Figure 1 shows the number of unique configurations for the various $Ni_{1-x}Al_x$ bimetallic phases over a temperature range of 0.1K – 1200K. Figure 1(a) shows the number of unique configurations with a probability of existence higher than 0%. The number of unique configurations increases in a sigmoidal trend as the temperature increases and reaches a plateau when the maximum number of unique configurations above 0% existence probability is reached. In Figure 1(a), the data can be divided into three temperature ranges. The first is from 0K – 200K; in this temperature range for most $Ni_{1-x}Alx$ bimetallic phases, there is a gradual increase in the number of configurations. At 200K, the bimetallic phases outside the $Ni_{12}Al_4$ to Ni_4Al_{12} (with a Ni content of 81.25% to 18.75%) range reach their maximum number of unique configurations. The second temperature range is from 200K – 900K; there is a linear increase in the number of unique configurations in this temperature range. The final temperature range is from 900K – 1200K. In this temperature range, all the bimetallic phases in the $Ni_{12}Al_4$ to Ni_4Al_{12} range reach a plateau for the unique configurations. The plateaus indicate that at 900K, the maximum number of unique configurations is no longer influenced by temperature. It should also be noted that a high percentage of the unique configurations above 200K has a probability of existence of less than 1%.

Figure 1(b) shows the number of unique configurations with probabilities of existence ≥ 1% as the temperature increases. The bimetallic phases outside the $Ni_{12}Al_4$ to Ni_4Al_{12} range, reach their maximum number of unique configurations at much lower temperatures than the bimetallic phases in the $Ni_{12}Al_4$ to Ni_4Al_{12} range, as seen in Figure 1(a). None of the bimetallic phases in the $Ni_{12}Al_4$ to Ni_4Al_{12} range reach their maximum number of unique configurations in Figure 1(b). However, the bimetallic phases in the $Ni_{12}Al_4$ to $Ni4Al_{12}$ range have a higher number of unique configurations over the 600K - 1200K temperature range, than the bimetallic phases outside of this range. Since there are fewer unique configurations for all the Ni1-xAlx bimetallic phases, the influence of temperature on the number of unique configurations could be seen more clearly. Additionally, the influence of temperature on the existence probability of the two inverse ratio $Ni_{1-x}Al_x$ bimetallic phases, namely Ni_2Al_{14} and $Ni_{14}Al_2$ or Ni_3Al_{13} and $Ni_{13}Al_3$, is seen in Figure 1(b).

The number of unique configurations could be further reduced by increasing the probability of existence cut-off. Therefore, unique configurations with probabilities ≥ 10% will be considered in the rest of the paper.

3.3 Stability of configurations

Studies on high entropy alloys show that the larger the entropy of the substance, the greater the stability thereof.[26] This observation follows from the fact that higher entropies lead to lower Gibbs-free energies. Figure 2 shows the entropy for the unique configurations with a probability of existence cut-off of ≥ 10% relative to the Ni content at 700K. The unique configuration data shows a parabolic trend across the Ni content range, centred around the 1:1 atomic ratio. The entropy for the unique configurations over this range of temperatures shows the same parabolic relationship

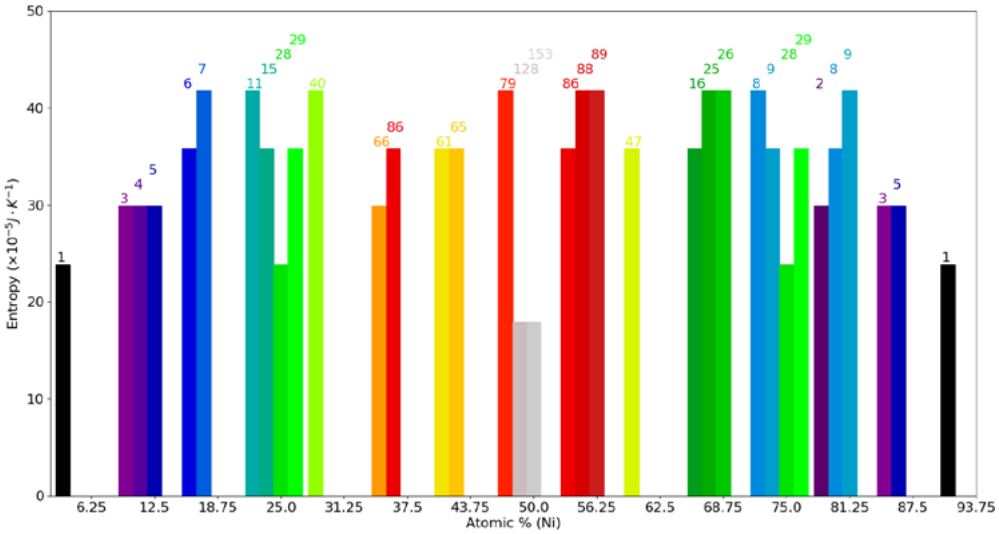

Figure 2: The entropy of the different configurations (the identifying number shown above the bar), with probabilities ≥ 10% relative to Ni content at 700K

with Ni content in the unique configurations as in Figure 2. The unique configurations with the highest entropy are in the 18.75% to 81.25% Ni content range for 700K. The ten configurations showing the highest entropies at 700K in Figure 2 are also seen at 800K. Additionally, 80% of these highest entropy configurations at 700K are also observed in the 600K – 1100K range. Entropy graphs for other temperatures over the entire 0.1K – 1200K range are available in the Supplementary Information.

The unique configurations of the bimetallic phases observed at 700K have an average Ni content of 20% - 80%. This range agrees with experimental studies showing the effective Raney nickel precursors to contain bimetallic phases in the 40% to 60% Ni range.[16,27]

Although ten unique configurations with the highest entropy were identified in Figure 2, the atomic arrangement of only eight of these configurations is shown in Figure 3 because the atomic arrangement in configurations 88 and 89 under Ni_9Al_7 and configurations 25 and 26 under $Ni_{11}Al_5$ are very similar, for each respective $Ni_{1-x}Al_x$ bimetallic phase. It is observed in Figure 3 (a) – (h) that there is a tendency of like-atoms to form clusters. This clustering tendency leads to patterns of non-homogeneous mixtures within the unique configurations.

The expectation is that the combination of non-homogeneous bimetallic phases will form a non-homogeneous bimetallic precursor. This non-homogeneity agrees with previous observations in literature.[28] The non-homogeneity of the bimetallic phases could be further investigated by calculating the enthalpy of mixing of

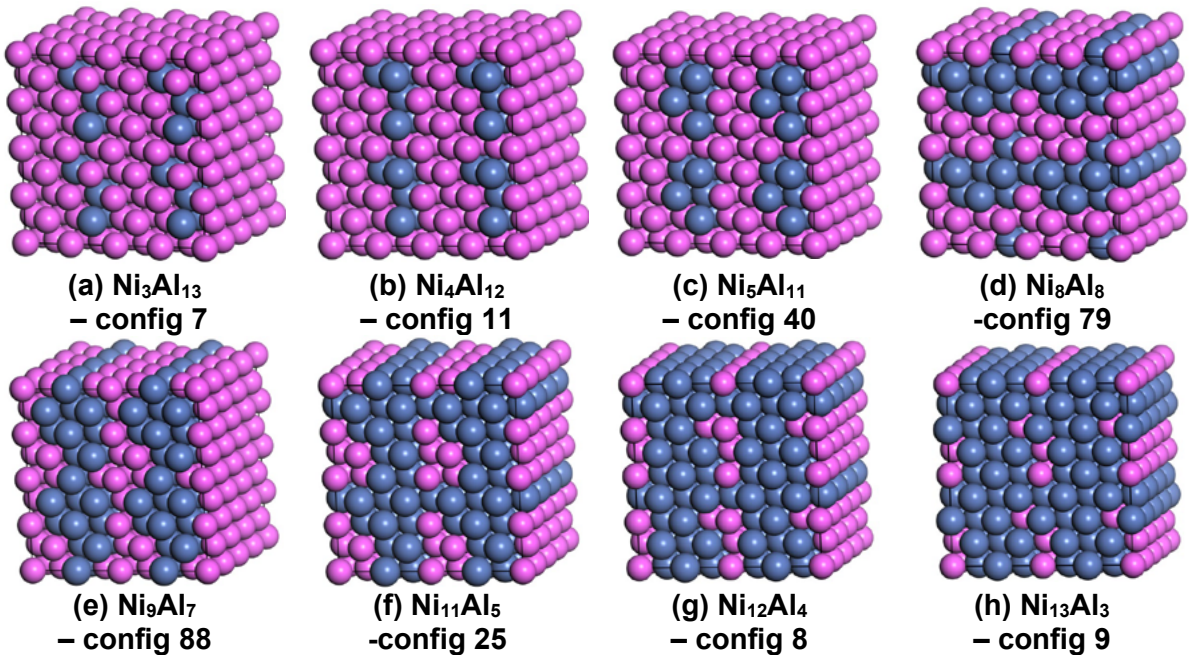

Figure 3: (a) - (h) The atomic structure of the unique configurations identified as most stable from entropy. (Al = magenta atoms and Ni = blue atoms.)

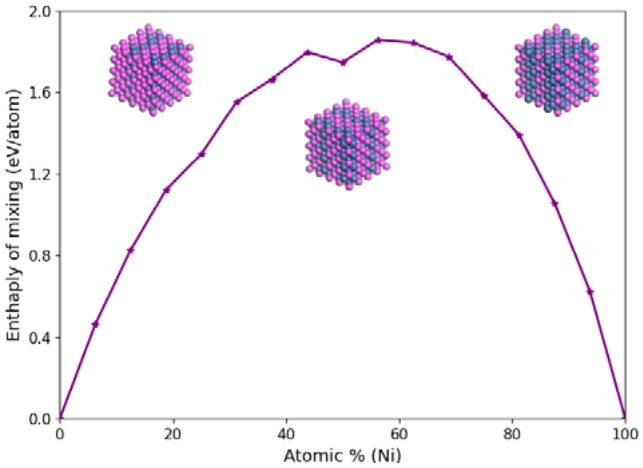

Figure 4: The enthalpy of mixing for $Ni_{1-x}Al_x$ bimetallic phases. The most stable configuration images of Ni_5Al_{11}, Ni_8Al_8 and $Ni_{11}Al_5$ are included

the bimetallic phases, as shown in equation (4). The enthalpy of mixing for the bimetallic phases is positive, as shown in Figure 4.

The positive enthalpy of mixing indicates that the bimetallic phases are chemically unmixed.[27,29] Chemical unmixing refers to the segregation of Ni and Al. This segregation leads to the formation of short-to-medium range chemical and topological order or clustering.[30] This observation supports the clustering observed in Figure 3. However, in the case of the 1:1 atomic ratio (bimetallic phase Ni_8Al_8), a slight decrease in the enthalpy of mixing is observed. While all the configurations of ratios surrounding the 1:1 atomic ratio show non-homogeneity, the configuration corresponding to the 1:1 ratio show a slightly more homogenous atomic arrangement (see inclusions in Figure 4), leading to a lower enthalpy of mixing.

4. Conclusion

In this study, a full spectrum of $Ni_{1-x}Al_x$ bimetallic phases was built using SOD. From the results, it can be concluded that using SOD to build the $Ni_{1-x}Al_x$ bimetallic phases led to the identifications of configurations that include the Ni content (40% - 60%) and agree with the non-homogeneity of Raney nickel precursors that have been used successfully in previous experimental and computational studies of OER.[14,19,28,29] Therefore, the SOD program provides a reliable spectrum of configurations that could be used for a more in-depth study of the influence of the precursor (containing various $Ni_{1-x}Al_x$ bimetallic phases) on the properties of Raney nickel. The next step in the study of Raney nickel will be to investigate the leaching of Al from the separate $Ni_{1-x}Al_x$ bimetallic phases or from a bimetallic precursor structure constructed by combining these $Ni_{1-x}Al_x$ bimetallic phases.

Supplementary information

Supplementary Information could be found at https://doi.org/10.25388/nwu.14626044

Acknowledgements

The financial assistance of the North-West University (NWU) and the National Research Foundation (NRF), under grant UID 117978, towards this research is hereby acknowledged. Opinions expressed and conclusions arrived at, are those of the authors and are not necessarily to be attributed to the NRF. Additionally, the authors would like to thank Jabus van den Berg for his technical support. This work was performed using the computational facilities of the Centre for High-Performance Computing (CHPC) of South Africa.

References

1. Coyle D. E and Simmons A. R 2014 *Understanding the Global Energy Crisis*
2. Demirbas A 2009 Global renewable energy projections *Energy Sources, Part B: Economics, Planning and Policy* **4** 212–24
3. Dresselhaus M S and Thomas I L 2001 Alternative energy technologies *Nature* **414** 332–7
4. Cheng Y and Jiang S P 2015 Advances in electrocatalysts for oxygen evolution reaction of water electrolysis-from metal oxides to carbon nanotubes *Progress in Natural Science: Materials International* **25** 545–53
5. Doyle R L and Lyons M E G 2016 The oxygen evolution reaction: mechanistic concepts and catalyst design *Photoelectrochemical solar fuel production* (Springer) pp 41–104
6. Santos D M F, Sequeira C A C and Figueiredo J L 2013 Hydrogen production by alkaline water electrolysis *Química Nova* **36** 1176–93
7. Lyu F, Wang Q, Choi S M and Yin Y 2019 Noble-Metal-Free Electrocatalysts for Oxygen Evolution *Small* **15** 1804201
8. Khan M A, Zhao H, Zou W, Chen Z, Cao W, Fang J, Xu J, Zhang L and Zhang J 2018 Recent progresses in electrocatalysts for water electrolysis *Electrochemical Energy Reviews* **1** 483–530
9. Colli A N, Girault H H and Battistel A 2019 Non-precious electrodes for practical alkaline water electrolysis *Materials* **12** 1336
10. Klein J C and Hercules D M 1981 Surface analysis of Raney nickel alloys *Analytical Chemistry* **53** 754–8
11. Zeifert B, Blásquez J S, Moreno J G C and Calderón H A 2008 Raney-nickel catalysts produced by mechanical alloying *Reviews on Advanced Materials Science* **18** 633–9
12. Tanaka S, Hirose N and Tanaki T 2000 Evaluation of Raney-nickel cathodes prepared with aluminum powder and tin powder *International Journal of Hydrogen Energy*
13. Devred F, Gieske A H, Adkins N, Dahlborg U, Bao C M, Calvo-Dahlborg M, Bakker J W and Nieuwenhuys B E 2009 Influence of phase composition and particle size of atomised Ni-Al alloy samples on the catalytic performance of Raney-type nickel catalysts *Applied Catalysis A: General* **356** 154–61
14. Schweizer S, Chaudret R, Low J and Subramanian L 2015 Molecular modeling and simulation of Raney Nickel: From alloy precursor to the final porous catalyst *Computational Materials Science* **99** 336–42
15. Schweizer S, Chaudret R, Spyriouni T, Low J and Subramanian L 2016 Influence of the Precursor Composition and Reaction Conditions on Raney-Nickel Catalytic System *Foundations of Molecular Modeling and Simulation: Select Papers from FOMMS 2015* ed R Q Snurr, C S Adjiman and D A Kofke (Singapore: Springer Singapore) pp 125–35
16. Divisek J, Mergel J and Schmitz H 1990 Advanced water electrolysis and catalyst stability under discontinuous operation *International Journal of Hydrogen Energy* **15** 105–14
17. Raney M 1940 Catalysts from alloys: Nickel Catalysts *Industrial and Engineering Chemistry* **32** 1199–203
18. Smith A J and Trimm D L 2005 The preparation of skeletal catalysts *Annual Review of Materials Research* **35** 127–42
19. Barnard N C and Brown S G R 2007 Kinetic Monte Carlo modelling the leaching of Raney Ni-Al alloys *WIT Transactions on Engineering Sciences* vol 54 pp 53–62
20. Barnard N C, Brown S G R, Devred F, Bakker J W, Nieuwenhuys B E and Adkins N J 2011 A quantitative investigation of the structure of Raney-Ni catalyst material using both computer simulation and experimental measurements *Journal of Catalysis* **281** 300–8
21. Grau-Crespo R, Hamad S, Catlow C R A R A and de Leeuw N H 2007 Symmetry-adapted configurational modelling of fractional site occupancy in solids *Journal of Physics: Condensed Matter* **19** 256201
22. Kimura Y, Qi Y, Cagin T and Goddard III W A 1998 *CALTECH ASCI TECHNICAL REPORT 003 The Quantum Sutton-Chen Many-Body Potential for Properties of fcc Metals*
23. Gale J D and Rohl A L 2003 The general utility lattice program (GULP) *Molecular Simulation* **29** 291–341
24. Anon Technical data for the element Nickel in the Periodic Table *https://periodictable.com/Elements/028/data.html* (accessed Oct 15, 2020)

25. Wang Q, Grau-Crespo R and de Leeuw N H 2011 Mixing thermodynamics of the calcite-structured (Mn,Ca)CO3 solid solution: A computer simulation study *Journal of Physical Chemistry B* **115** 13854–61
26. Zhang Y 2019 *High-Entropy Materials* (Singapore: Springer Singapore)
27. Manzoor A, Pandey S, Chakraborty D, Phillpot S R and Aidhy D S 2018 Entropy contributions to phase stability in binary random solid solutions *npj Computational Materials* **4**
28. Lee G D, Suh C S, Park J H, Park S S and Hong S S 2005 Raney Ni catalysts derived from different alloy precursors (I) morphology and characterization *Korean Journal of Chemical Engineering* **22** 375–81
29. Fultz B 2010 Vibrational thermodynamics of materials *Progress in Materials Science* **55** 247–352
30. MA E 2005 Alloys created between immiscible elements *Progress in Materials Science* **50**